


Article

Influence of Surface Sputtering during High-Intensity, Hot Ion Implantation on Deep Alloying of Martensitic Stainless Steel

Alexander Ryabchikov *, Olga Korneva, Anna Ivanova, Sergey Dektyarev , Dimitriy Vakhrushev and Alexander Gurulev

Research School of High-Energy Physics, National Research Tomsk Polytechnic University, 30 Lenin Ave., 634050 Tomsk, Russia; oskar@tpu.ru (O.K.); bai@tpu.ru (A.I.); dektyarev@tpu.ru (S.D.); dov3@tpu.ru (D.V.); avg72@tpu.ru (A.G.)

* Correspondence: ralex@tpu.ru; Tel.: +7-(913)-820-41-80

Abstract: This article is devoted to the study of the effect of ion sputtering on the alloy surface, using the example of martensitic stainless steel AISI 420 with ultrahigh-dose, high-intensity nitrogen ion implantation on the efficiency of accumulation and transformation of the depth distribution of dopants. Some patterns of change in the depth of ion doping depending on the target temperature in the range from 400 to 650 °C, current density from 55 to 250 mA/cm², and ion fluence up to 4.5×10^{21} ion/cm² are studied. It has been experimentally established that a decrease in the ion sputtering coefficient of the surface due to a decrease in the energy of nitrogen ions from 1600 to 350 eV, while maintaining the ion current density, ion irradiation fluence and temperature mode of target irradiation increases the ion-doped layer depth by more than three times from 25 µm to 65 µm. The efficient diffusion coefficient at an ion doping depth of 65 µm is many times greater than the data obtained when stainless steel is nitrided with an ion flux with a current density of about 2 mA/cm².

Keywords: martensitic stainless steel; ultrahigh-dose; high-intensity ion implantation; ion surface sputtering; depth of ion doping



Citation: Ryabchikov, A.; Korneva, O.; Ivanova, A.; Dektyarev, S.; Vakhrushev, D.; Gurulev, A. Influence of Surface Sputtering during High-Intensity, Hot Ion Implantation on Deep Alloying of Martensitic Stainless Steel. *Metals* **2023**, *13*, 1604. <https://doi.org/10.3390/met13091604>

Academic Editors: Matteo Benedetti and Francesca Borgioli

Received: 28 July 2023

Revised: 8 September 2023

Accepted: 13 September 2023

Published: 16 September 2023



Copyright: © 2023 by the authors. Licensee MDPI, Basel, Switzerland. This article is an open access article distributed under the terms and conditions of the Creative Commons Attribution (CC BY) license (<https://creativecommons.org/licenses/by/4.0/>).

1. Introduction

In many cases, the material's surface and near-surface layers are responsible for the operational properties of products made of metals and alloys. With this background, the development of methods for improving the microstructure and surface properties is of great importance. Among the variety of methods, a special place is occupied by the beam-plasma processing of materials. At that, three directions can be distinguished, which differ in the physical principles of modifying the elemental composition, microstructure, and surface properties. The most widespread methods are ion-plasma deposition of coatings, such as physical vapor deposition and magnetron sputtering [1–4]. With all their advantages, due to the wide possibilities of plasma deposition of coatings, these methods have a disadvantage caused by the fundamentally unsolvable problems of coatings delamination [5]. Alternative methods for modifying the near-surface properties of metals and alloys are based on the energy impact on the surface. The impact of laser radiation [6], high-current electron beam [7], powerful plasma fluxes [8], or powerful ion beams [9,10] is based on pulsed heating of the surface layer, up to melting and even evaporation, followed by ultrafast heat transfer into the material due to its thermal conductivity.

Ion modification of materials has a number of advantages over other methods. This method allows you to controllably change the elemental and phase compositions and, as a result, provide a controlled change in the microstructure and properties of various materials [11–14]. Figure 1 shows a diagram defining the areas of various ion implantation methods, including beamline ion implantation, plasma-immersion ion implantation, low-energy high-current ion implantation, low-energy high-intensity ion implantation, a

method based on the synergy of high-intensity ion implantation and energy impact on the surface and high-intensity ion beam material modification. The main disadvantage of the ion implantation methods is associated with the short range of ions in a solid, usually not exceeding several tens or hundreds of nanometers. Changing the thickness of the ion-doped layer due to an increase in ion energy, including through the use of multiply charged ions, is ineffective and leads to the complication of installations for ion implantation and increases the cost of ion-beam processing of materials [15,16].

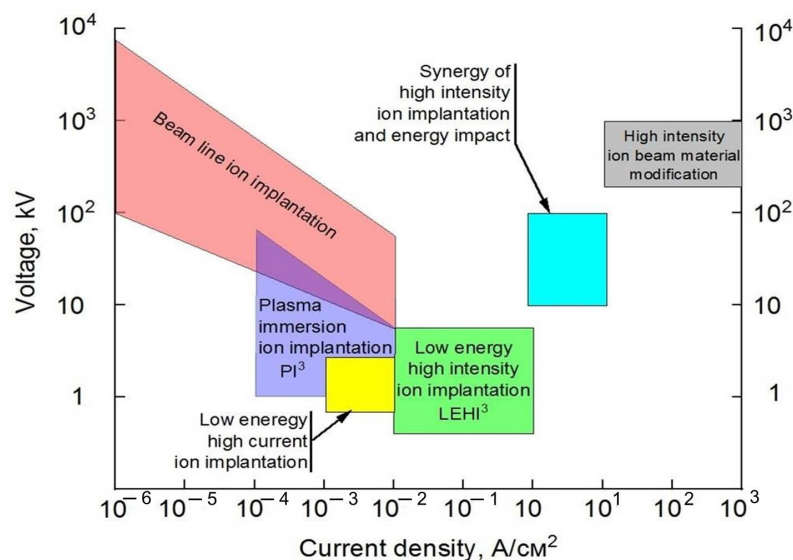


Figure 1. Diagram defining the areas of various ion implantation methods.

The method of synergy of high-intensity implantation and the energy impact of submillisecond high-power density ion beams on the surface (Figure 1), recently proposed in [17], suggests a solution to the problem of possible surface overheating due to high power densities of the ion current. The method involves the application of repetitively-pulsed heating of the near-surface layer of metals and alloys to temperatures providing radiation-enhanced diffusion of dopants. Pulsed heating of the near-surface layer, combined with rapid heat transfer into the material, due to its thermal conductivity, decreases the temperature in the irradiated material volume.

The high-intensity ion beam material modification method (Figure 1) is implemented at ion current densities from 10 to 10^3 A/cm² and accelerating voltages from 100 to 1000 kV [9,10]. Such ion beams with a pulse duration of several tens, and sometimes hundreds of nanoseconds, provide energy input to the near-surface layer when the surface is superfast heated to temperatures corresponding to the melting and even evaporation of the irradiated target material. Ultra-fast surface layer cooling provides the over-hardening effect of the irradiated materials. The nanosecond duration and low frequency of high-power ion accelerator pulses make it possible to use them for implantation only at very low ion irradiation fluences.

Wei et al. [18–20] and Hutchings [21] were the first to show the possibility of significantly increasing the diffusion of nitrogen into various steels when the ion current density increases to 5 mA/cm². A significant increase in the current density of nitrogen ions, even at an ion energy of about 1 keV, made it possible to carry out ion implantation at elevated temperatures, providing a significant increase in radiation-enhanced dopant diffusion. Thanks to high-current ion implantation modes, the surfaces of metal samples were effectively cleaned of oxides and carbides that block nitrogen diffusion. High-current implantation of nitrogen ions with an energy of 1 keV and a current density of about 2 mA/cm² for two hours made it possible to form an ion-alloyed layer in martensitic steel up to 20 μm thick. In general, based on a set of studies carried out in [18–23], a significant influence of the ion current density on the penetration depth of dopants was confirmed. At a low ion current density, the diffusion process can be blocked by forming an oxide or

carbon film on the irradiated surface, which is deposited from the residual atmosphere of the vacuum chamber. Increasing the ion current density to several milliamperes per square centimeter ensures the sputtering of the oxide-carbon film, stimulating the diffusion of implanted atoms.

In [24], the possibility of increasing the ion current density of a pulse-periodic beam of low-energy ions through the use of a ballistic focusing system to several tens and hundreds of milliamperes per square centimeter was first shown. This stimulated a new round of research on high-intensity low-energy ion implantation (Figure 1). An increase in the ion current density by several orders of magnitude provided a corresponding increase in the ion implantation fluence and, as a result, expanded the possibilities of forming deep ion-doped layers in metals and alloys at short times of ion-beam processing of materials. However, at ion implantation fluences at the level of 10^{20} – 10^{21} ion/cm², required for deep ion doping of metals and alloys, the ion sputtering of the irradiated material's surface layer becomes significant. Surface sputtering, in turn, reduces the efficiency of dopant accumulation in the substance, since the previously implanted atoms are sputtered together with the sputtering of the matrix substance of the target. The thicknesses of ion-doped layers should ultimately be determined by the competition of radiation-enhanced diffusion of implanted atoms and ion sputtering of the surface. Ion sputtering of the surface at low current densities not exceeding several milliamps per square centimeter has been sufficiently well studied. It is also known that at ion current densities of tens and hundreds of amperes per square centimeter, even with the nanosecond pulse duration of a high-power pulsed beam, ion sputtering is combined with evaporation of the surface layer. At current densities of low energy ions of hundreds of milliamps per square centimeter with a microsecond-submillisecond duration, the ion irradiation fluence in each pulse can vary from 10^{13} – 10^{16} ion/cm². Each implanted ion causes a cascade of displacements of target atoms. The displacement density of atoms in the implanted layer can approach the density of atoms in metals and alloys. This can affect both ion sputtering and atomic diffusion. For example, in [18] a model was proposed that allows the emergence at such parameters of ion implantation of a shock-wave mechanism of mass transfer of dopants, which would significantly change the diffusion coefficient. Detailed studies of the effect of high-intensity implantation of ions, including low-energy nitrogen ions, on the patterns of ion sputtering of metals and alloys and the diffusion coefficient have not been carried out so far.

As in Wei's works [19,20], AISI420 steel was used for high-intensity nitrogen implantation.

The article considers the influence of ion sputtering on the surface during high-dose, high-intensity nitrogen ion implantation on the accumulation efficiency, spatial distribution and diffusion coefficient in steel AISI 420, widely used in various fields of science and technology. The regularities of ion sputtering in steel AISI 420 are studied depending on the ion current density and ion irradiation fluence. The possibility of increasing the accumulation efficiency of implanted atoms during high-intensity ion implantation due to various methods of reducing the ion sputtering of the surface of the irradiated target is studied.

2. Materials and Methods

The studies were carried out on a complex installation for ion-beam and plasma processing of materials, the diagram of which is presented in Figure 2. The ultimate vacuum with a pressure of about 10^{-3} Pa was achieved using turbomolecular high-vacuum and spiral forevacuum pumps. To generate nitrogen plasma using a gas-discharge source PINK [25], nitrogen was filled into the chamber to a pressure of 0.4 Pa. The formation of gas-discharge plasma was carried out at an arc discharge current of 25 A.

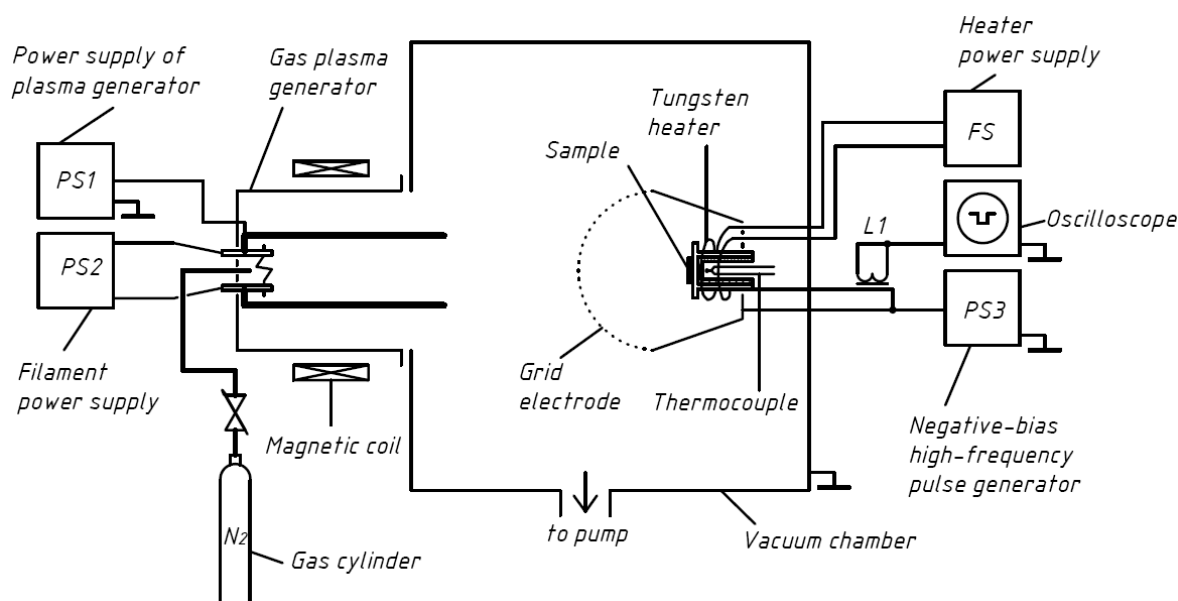


Figure 2. Scheme of the experimental installation.

As in the case of a beam of metal ions [24], the repetitively-pulsed formation of nitrogen ions was carried out using plasma-immersion extraction, subsequent acceleration and transportation of the beam in the equipotential drift space with ballistic focusing of ions. A grid extractor with a radius of 7.5 cm had a cell size of 1.2×1.3 mm. The samples were irradiated with a beam of nitrogen ions with an energy of singly charged nitrogen ions up to 1.6 keV at a pulse duration of 4 μ s and a frequency of 10^5 pulses/s. Specimens for irradiation are made of AISI 420 steel. AISI 420 steel refers to martensitic stainless steel with a hardening temperature of about 1050 °C followed by tempering at about 280 °C. The steel contains about 13% of chromium, and less than 0.6% of silicon, manganese and nickel. The content of sulfur and phosphorus is less than 0.03%. The microhardness of the original specimen was about 3 GPa. In the process of ion beam treatment, martensitic steel samples with a height of 5 mm and a radius of 10 mm were preheated with an ion beam to a temperature of 500 °C. The heating time at an ion current density of 250 mA/cm² was about 20 min. The ion current of a collector was measured using a current transformer (L1), whose signals were recorded using a Le Croy oscilloscope.

With a decrease in the ion current density, the specimen was heated using an additional heater in order to achieve the required temperature. The temperature of the specimen during irradiation was measured by an isolated thermocouple.

The diffractograms of the specimens under investigation by X-ray diffraction analysis on a DRON-7 diffractometer were taken with continuous 2 θ scanning with Bragg–Brentano focusing in the cobalt anode radiation (radiation wavelength Co K α λ = 0.1789 nm).

A cross-section of the specimens and scanning electron microscopy were used to determine the thickness of the ion-doped layer. The thicknesses of the ion-sputtered layers were studied using a profilometer Micro Measure 3D Station. The study of hardness was carried out on a microhardness tester KV 5S WP-FA according to the Vickers method at a load of 50 mN. Tribological studies were carried out on a PC-Operated High Temperature Tribometer TNT-S-AX0000 in the dry friction mode using the “ball-indenter-rotating disk” method. The wear test was carried out at a fixed sample rotation speed of 2 cm/s with an indenter load of 5 N. The number of cycles (passed revolutions) was 3500, which is equal to 35 m. An Al₂O₃ ball with a diameter of 3 mm was used as an indenter. The wear resistance of the samples was evaluated by the cross-sectional area of the wear track after tribological tests, scanned on a three-dimensional non-contact profilometer Micro Measure 3D Station.

3. Experimental Results and Discussion

For the deep ion doping of metals and alloys, it is necessary to increase the fluences of ion irradiation by several orders of magnitude compared to traditional methods of ion-beam processing. The solution to this problem due to the time of ion implantation will lead to the fact that the processing of the product will have to be carried out for several days. An alternative option implies an increase in the ion irradiation fluence due to an increase in the ion current density. Figure 3a shows the distributions of the introduced nitrogen concentration in specimens irradiated with a beam of nitrogen ions with a current density of 120 mA/cm² when the irradiation fluence changes from 3.6×10^{20} ion/cm² to 2.2×10^{21} ion/cm² due to an increase in the ion implantation time from 20 min to 120 min.

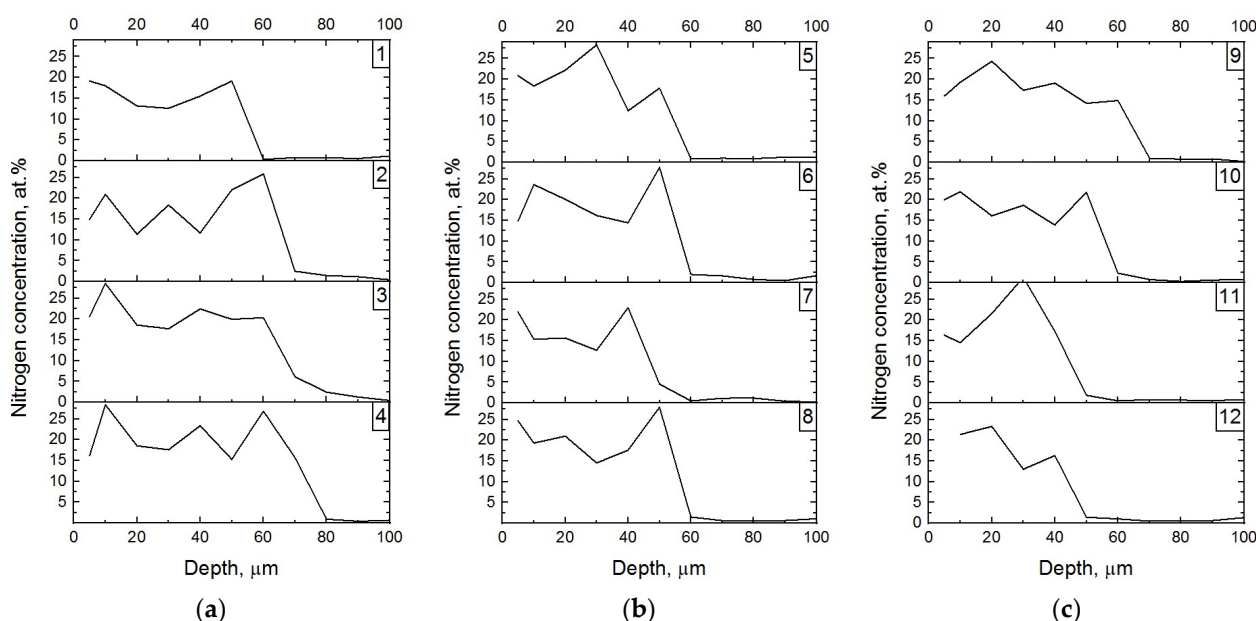


Figure 3. Influence of the ion current density ((a)—120 mA/cm²; (b)—155 mA/cm²; (c)—230 mA/cm²) and the fluence of ion irradiation: ion/cm² (1— 3.6×10^{20} , 2— 1.1×10^{21} , 3— 1.65×10^{21} , 4— 2.2×10^{21} ; 5— 4.8×10^{20} ; 6— 1.4×10^{21} ; 7— 2.1×10^{21} ; 8— 2.9×10^{21} ; 9— 7.1×10^{20} ; 10— 2.1×10^{21} ; 11— 3.15×10^{21} , 12— 4.3×10^{21}) on the depth distribution of nitrogen.

An increase in the fluence of ion irradiation gradually increases the depth of ion doping due to the radiation-enhanced diffusion of dopants. The depth of ion doping reaches 60 μm at an ion fluence of 3.6×10^{20} ion/cm². An increase in the ion fluence by a factor of three to 1.1×10^{21} ion/cm² is accompanied by an increase in the penetration depth of nitrogen to 70 μm. A further doubling of the ion irradiation fluence to 2.2×10^{21} ion/cm² also increases the thickness of the doped layer by about 10 μm more. The maximum nitrogen concentration can reach 30 at%. These data unequivocally indicate a disproportionate dependence of the increase in the thickness of the ion-doped layer on the fluence of steel irradiation with nitrogen ions. The highest growth rate of the modified layer thickness occurs during the first 20 min of high-intensity implantation of nitrogen ions. Taking into account that the diffusion of nitrogen into the target depth also occurs during the dynamic heating of the specimen to the required temperature, including by the ion beam, the observed initial growth rate of the doped layer thickness will be somewhat less than 180 μm/h.

With an increase in the ion current density to 155 mA/cm² and an ion irradiation fluence to 4.8×10^{20} ion/cm², the depth of the ion-doped layer did not change compared to 20 min irradiation at a lower ion current density (Figure 3b, curve 1). It is characteristic that a further increase in the ion irradiation fluence due to a six-fold increase in the ion implantation time to 2.9×10^{21} ion/cm² is not accompanied by a noticeable change in the

distribution profile of the implanted nitrogen over the depth of the specimen (Figure 3b, curves 6, 7, 8).

A further increase in the nitrogen ion current density to 230 mA/cm² changes the dynamics of the formation of a deep ion-doped layer (Figure 3c). At an initial fluence of ion irradiation of about 7.1×10^{20} ion/cm², the thickness of the ion-doped layer turned out to be approximately the same as at the other two ion current densities, but with smaller ion fluences. However, the growth of the ion irradiation fluence to almost 4.3×10^{21} ion/cm² did not increase but decreased the thickness of the ion-doped layer (Figure 3c, curve 12).

A comparative analysis of the data in Figure 3 a–c clearly demonstrates a decrease in the thickness of the ion-doped layer with an increase in the ion current density, especially at high ion irradiation fluences. Such a dependence on the thickness of the ion-doped layer cannot be explained only by the influence of radiation-enhanced diffusion of nitrogen atoms with a change in the ion current density and ion irradiation fluence. Their growth should be accompanied by an increase in the penetration depth of nitrogen ions. It is obvious that there is a competing factor limiting the thickness growth of the ion-doped layer during the high-intensity implantation of ions into metals and alloys.

Ion sputtering of the surface may be among the most significant factors. According to [26], the thickness of the ion-modified layer h is directly proportional to the diffusion coefficient of nitrogen D and inversely proportional to the ion sputtering rate of the surface of the metal and alloy V , and it is determined by a simple expression:

$$h = 2D/V \quad (1)$$

With respect to implantation by repetitively-pulsed ion beams, this formula takes the form:

$$h = 2D/j_i \times f \times \tau \times S \quad (2)$$

where j_i is ion current density; f is ion beam pulse frequency; τ is ion beam pulse duration; S is ion sputtering ratio of a solid surface.

In traditional implantation, when the ion irradiation fluence is usually 2×10^{17} ion/cm², the thickness of the ion-sputtered layer of the irradiated target is not greater than 0.1 μ m. On the one hand, this is a small amount. On the other hand, it does have a significant influence on the accumulation and formation dynamics of the distribution profile of the dopants. This is caused by the fact that the ion sources forming ion beams with energy not greater than 100 keV are used for the conventional ion implantation into metals and alloys. The projective range of such ions in a solid is several tens of nanometers. Thus, the thickness of the ion-sputtered surface layer of the implantable target increases with the increase in ion irradiation fluence. Ultimately, ion sputtering limits the concentrations of dopants (N_d) to a level determined by the following expression:

$$N_d = N_0/S \quad (3)$$

where N_0 is the atomic density of matter.

At ion energies from 50 to 100 keV, the maximum level of the achieved dopant concentration usually does not exceed (25–35) at%. To compensate for ion sputtering in the repetitively-pulsed mode of ion implantation, the plasma deposition of a thin coating was used in the intervals between pulses of ion irradiation of the surface. A single source with a continuous vacuum arc discharge was used to generate a metal ion beam and to deposit a metal plasma. The possibility of implementing the mode of high-concentration implantation was achieved due to the fact that the plasma deposition duration could exceed the duration of ion beam formation by one or two orders of magnitude.

In the case of high-intensity implantation with a significant decrease in the ion energy, the ion sputtering coefficient should decrease significantly. At the same time, an increase in the ion irradiation fluence by several orders of magnitude can have a significant influence on the dynamics of the accumulation of implanted atoms, the depth of ion doping of metals and alloys, and surface morphology.

Initially, the influence of the temperature of an irradiated specimen made of steel AISI 420 on the depth distribution of implanted nitrogen was studied. Implantation was carried out at an ion energy of 1.5 keV and a current density of 160 mA/cm². Figure 4 shows the depth distribution profiles of the nitrogen concentration of the implanted target. The layer thickness approaches 50 µm, and the concentration reaches almost 25 at.% at a specimen temperature of 450 °C. At temperatures from 500 to 550 °C, the maximum concentration remains stable, and the layer thickness reaches 60 µm. It is important to note that an increase in the target temperature to 650 °C was accompanied by an almost complete release of nitrogen gas from the implanted target.

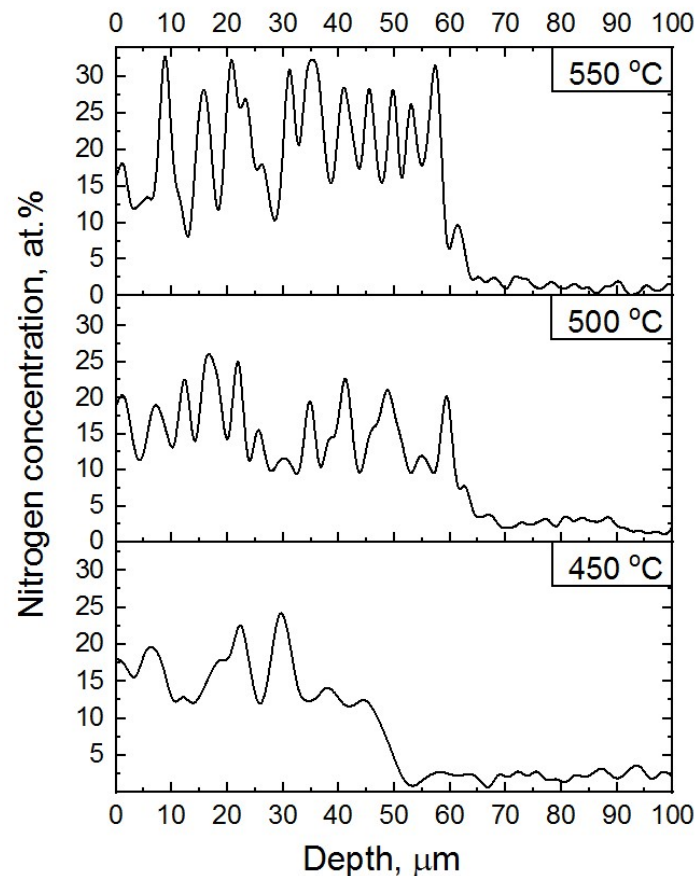


Figure 4. Concentration profiles of depth distribution of nitrogen dopant for specimen of steel AISI 420 modified at different temperatures.

The results of a study on the martensitic steel specimen phase composition after nitrogen implantation by the method of X-ray diffraction analysis are presented in Figure 5. The data of Figure 5 show fragments of X-ray patterns of martensitic steel sample after nitrogen ion implantation at $T = 500$ °C, obtained by a symmetric scheme for taking in cobalt $K\alpha$ -radiation. A surface-modified layer contains the matrix α -phase (α -Fe), iron nitride Fe_4N (γ' -phase), and chromium nitride CrN. The calculation of the relative number of formed phases showed that the modified layer has the following composition: α -phase–70.88 vol.%, γ' - Fe_4N –16.30 vol.%, CrN–12.82 vol.%.

According to the data on the temperature dependence of the ion-doped layer parameters, the regularities of ion sputtering were studied at a specimen temperature of 500 °C and ion energy in the beam 1.2 keV. Figure 6 shows the dependence of the ion-sputtered layer thickness on the current density of nitrogen ions after irradiation of the specimen for two hours.

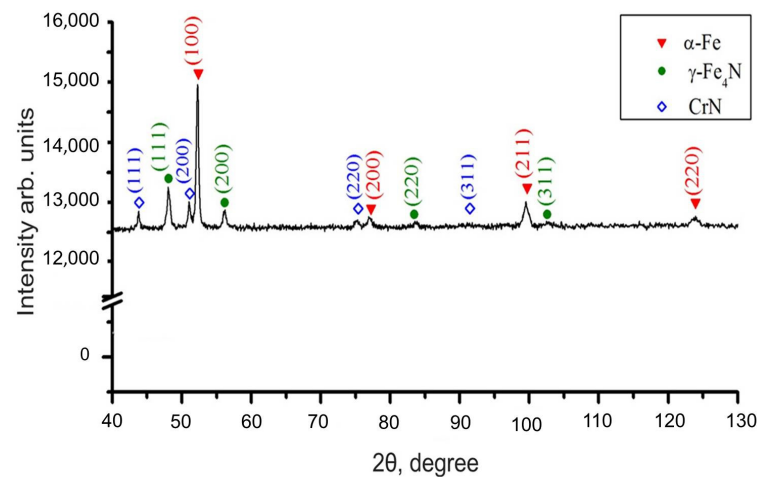


Figure 5. Fragments of X-ray patterns of martensitic steel sample after nitrogen ion implantation at $T = 500\text{ }^{\circ}\text{C}$.

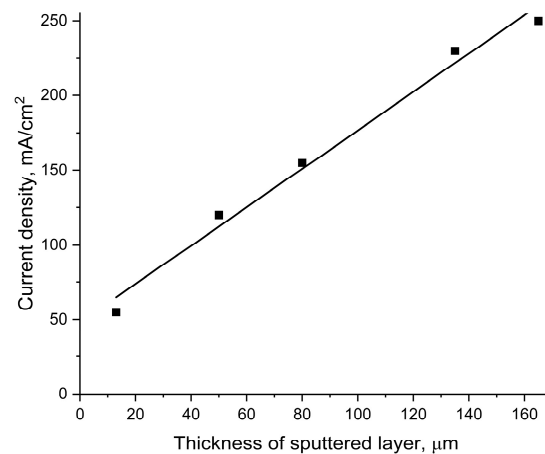


Figure 6. The dependence of the ion-sputtered layer thickness on the ion current density at an irradiation time of 2 h.

The sputtered layer thickness increases from $12\text{ }\mu\text{m}$ to about $165\text{ }\mu\text{m}$ as the ion current density increases from 55 mA/cm^2 to 250 mA/cm^2 . The dependence is practically linear. This indicates that in this range of current densities, the collective effects inherent in the impact of high-power ion beams on the surface of a solid do not manifest when even evaporation of the surface layer can take place. Ion sputtering increases in proportion to the increase in the ion irradiation fluence, which depends on the ion current density in accordance with the expression:

$$\Phi = j_i \times f \times \tau \times t/e \quad (4)$$

where t is the time of ion implantation and e is the electron charge. It should be taken into account that the total irradiation time t includes the pretreatment time t_p of 20 min and the ion implantation time t_0 . Thus, the ion irradiation fluence and, accordingly, the ion sputtering depth increases due to the ion pretreatment of the target by k times, where k :

$$k = \frac{t_p}{t_p + t_0} \quad (5)$$

It can be seen from expression 4 that the ion irradiation fluence can also be controlled by changing the ion irradiation time. Figure 7 shows the research results carried out at a constant average pulsed ion current density of 250 mA/cm^2 .

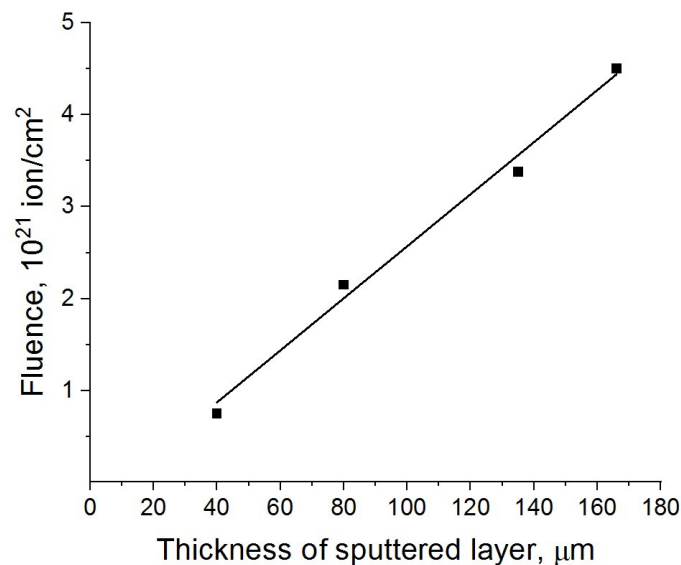


Figure 7. Dependence of the ion-sputtered layer thickness on the fluence of irradiation of the specimen made of steel AISI 420 with nitrogen ions.

The average pulsed ion current density was determined by averaging 1024 pulses using the mathematical apparatus of a Le Croy oscilloscope. As can be seen from the data in Figure 7, the change in the ion irradiation fluence from $7.5 \times 10^{20} \text{ ion/cm}^2$ to $4.5 \times 10^{21} \text{ ion/cm}^2$ increased the thickness of the ion-sputtered layer from 36 to 166 μm . Thus, the maximum surface sputtering rate in these experiments reached 83 μm per hour.

The ion sputtering rate is directly proportional to the ion current density j_i and the ion sputtering coefficient S [27]. The coefficient of sputtering of polycrystalline materials by ions with energies of about 1 keV is determined by the following expression [28]:

$$S = 0.15 \cdot \alpha \cdot \frac{M_i \cdot M_a \cdot E_i}{E_s \cdot (M_i + M_a)^2} \quad (6)$$

where M_i and M_a are atomic masses of ions and atoms of the target, g/mol; E_i is the energy of incident ions, eV; E_s is the sublimation energy of target atoms, eV; α is a dimensionless parameter depending on M_i/M_a .

The presented experimental data show that the depth of ion doping of metals and alloys during high-intensity repetitively-pulsed implantation is determined by the competition of radiation-enhanced diffusion of dopants and sputtering of the surface layer of the implanted material. Ion sputtering of the surface reduces the growth rate of the ion-doped layer, limits its maximum thickness, and can significantly affect the relief and surface morphology. Moreover, the surface sputtering at significant fluences of ion irradiation significantly affects the efficiency of dopant accumulation and increases the cost of ion-beam processing of the material. For example, at an ion irradiation fluence of $4.5 \times 10^{21} \text{ ion cm}^{-2}$, the thickness of the ion-sputtered layer was 166 μm , while the depth of ion doping was only about 50 μm . At the beginning of ion implantation, the target material is sputtered. However, at low ion energy, the near-surface layer is quickly saturated with the implanted material. After that, the sputtering of the surface is accompanied by the simultaneous sputtering of the previously introduced atoms. Based on the data on the thickness of the modified and sputtered layers, it can be concluded that, finally, only 23% of the implanted nitrogen atoms were accumulated in the modified layer; 77% of the implanted atoms were removed during ion implantation due to ion sputtering of the surface. In the case of nitrogen ion implantation, such losses do not have a significant effect on the cost characteristics of modifying the microstructure and properties of metals and alloys. However, if expensive dopants are used for implantation, significant sputtering can also affect the cost of materials property modification. In this regard, studying possible methods

for reducing the ion sputtering of the surface of metals and alloys during super-high-dose, high-intensity implantation of low-energy ions is of fundamental importance.

Taking into account the high rates of ion sputtering of the irradiated surface during high-intensity implantation, it becomes obvious that it is practically impossible to use the deposition of metal plasma purified from the microdroplet fraction to compensate for ion sputtering. The option of reducing the sputtering of the solid surface due to reducing the energy of the ions seems more attractive. It follows from expression 4 that the ion sputtering coefficient decreases in proportion to the decrease in the ion energy. In [23], the possibility of forming high-intensity beams with a current density of tens and even hundreds of milliamperes per square centimeter at energies of gas and metal ions of about 400 V is shown. Two variants of ion beam extraction with subsequent ballistic focusing of ions have been studied. It is shown that in the case of using a single-grid extractor, the decrease in the ion energy is limited by the ratio of the high voltage sheath width and the grid cell size. At potentials when the layer width becomes comparable with the grid cell size, the free ion-emission plasma boundary is deformed and a significant part of the ion flux, accelerated in the sheath layer, falls on the grid structure elements. The best beam characteristics were obtained using a two-grid system implementing a combination of ion acceleration followed by partial deceleration. A potential with an amplitude of 1200 to 1600 V is applied to the grid closest to the plasma, at which the sheath layer width is several times greater than the grid cell size. This creates good conditions for forming an ion beam at the entrance to the drift space. The second grid provides a decrease in the ion energy to values determined by the potential amplitude of this grid.

The effect of nitrogen ion energy under conditions of reduced ion sputtering of the surface of steel AISI 420 was studied at fixed parameters, such as target temperature, ion implantation fluence and irradiation time. The temperature mode of ion irradiation with varying ion energy was maintained due to a corresponding change in the bias potential pulse duration at a fixed frequency.

Figure 8 demonstrates the fundamental possibility of increasing the thickness of the ion-modified layer by suppressing ion sputtering. The ion beam was formed by a single-grid system in the plasma-immersion mode. Irradiation of a specimen of AISI 420 steel for one hour at a temperature of 400 °C with a nitrogen ion beam with an energy of 1600 eV leads to the formation of an ion-doped layer with a thickness of about 25 µm. A decrease in the ion energy to 950 eV at the same temperature and maintaining the fluence is accompanied by a decrease in the maximum depth of ion sputtering of the surface layer from 60 µm to 22 µm. As can be seen from Figure 8, in this case, the layer thickness increases to approximately 40 microns. A further decrease in the ion energy to 350 eV almost completely suppresses the ion sputtering of the surface. The thickness of the sputtered layer in this case was not greater than 4 µm.

As shown in Figure 8a,b the width of the ion-doped layer reaches 65 µm. The depth distribution of nitrogen concentration correlates well with the metallographic analysis data.

Figure 9 shows the results of studying the change in microhardness over the depth of the specimen irradiated at a bias potential amplitude of 350 V. The data in the figure show that the microhardness of the specimen after irradiation increased by about 1.7 times. The depth distribution of microhardness correlates quite well with the distribution of nitrogen (Figure 9).

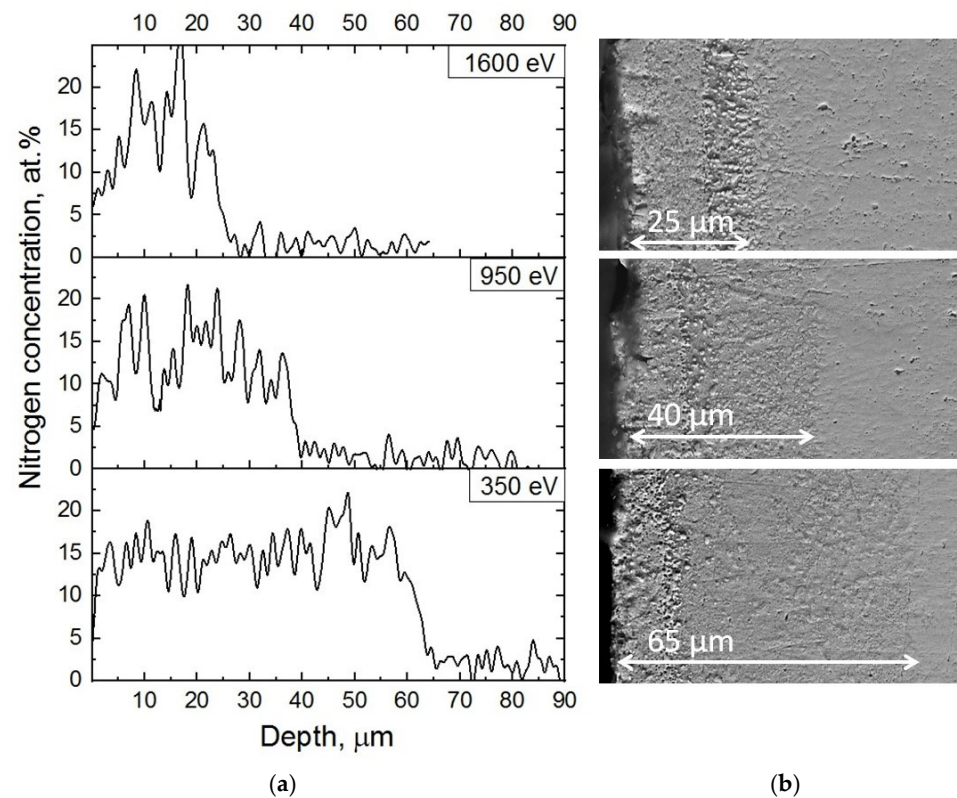


Figure 8. Nitrogen distribution profiles (a) and micrographs of the cross-section (b) depending on the ion energy.

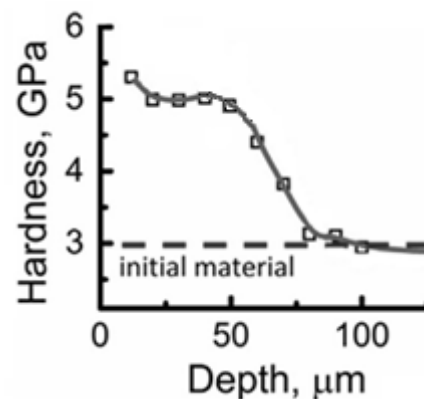


Figure 9. Distribution of microhardness along the depth of an ion-doped sample.

Figure 10 shows the dependence of the friction coefficient curves on the indenter run length for the original steel specimen (1) and the modified specimen (2). First, the friction coefficient for the original steel AISI 420 increases sharply, i.e., passes the way of running in the surface layer of the specimen and the counter-body, and then it reaches a plateau with a stable average friction coefficient equal to 0.84. On curve 2, the nature of the change in the friction coefficient changes, and the traveled distance is divided into three sections. A smooth increase in the friction coefficient is the way of wear of the nitrided layer, a sharp increase in the friction coefficient is, perhaps, due to a change in the structure or phase composition of the layer and reaching a plateau with a value equal to the friction coefficient of the original specimen.

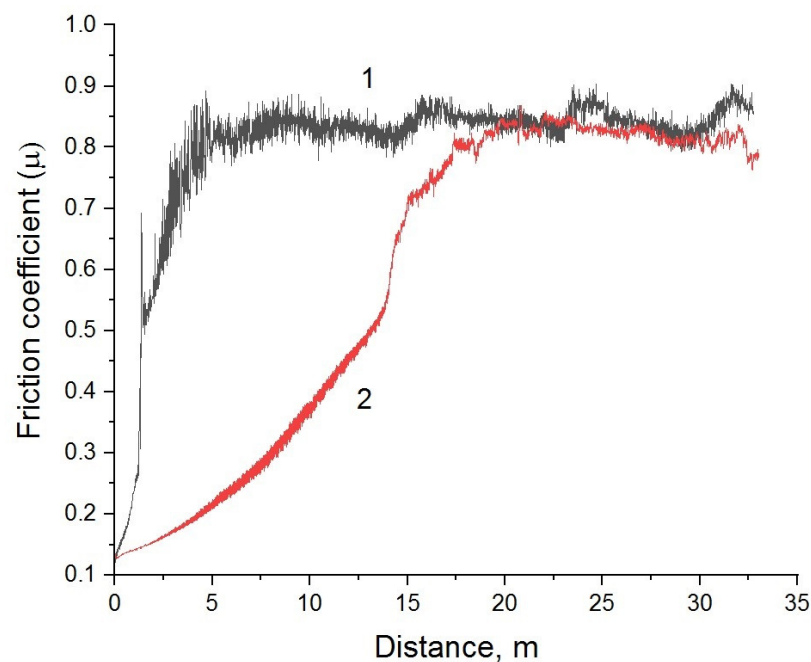


Figure 10. Dependence of the friction coefficient on the length of the indenter run: 1—for the original steel AISI 420, 2—implanted with nitrogen ions.

Figure 11a,b shows 3D images of wear tracks and characteristic profiles of wear tracks. The depth and average area of the wear track for the original specimen were $50\text{ }\mu\text{m}$ and $26,000\text{ }\mu\text{m}^2$, respectively. For the modified specimen, the wear track depth is $1.6\text{ }\mu\text{m}$, and the track profile area is $160\text{ }\mu\text{m}^2$.

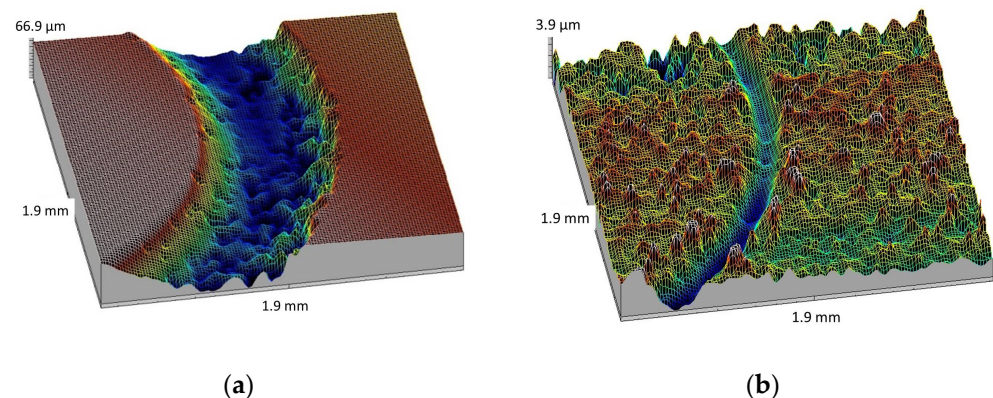


Figure 11. Three dimensional images of wear tracks: (a)—original specimen, (b)—implanted specimen.

The presented data show that the implantation of AISI 420 steel with high-intensity nitrogen beams significantly improves the physical and mechanical properties of the specimen surface and increases the hardness and wear resistance by 160 times.

Thus, the control of the ion sputtering of the surface during high-intensity ion implantation and ultrahigh fluences of ion irradiation of targets creates conditions for a significant variation in the depth of the ion-doped layer due to a change in the ion energy. It is also important to note that the surface morphology undergoes less change in this case.

The obtained experimental data qualitatively agree with theoretical concepts and confirm the possibility of a multiple increase in the thickness of the ion-doped layer during high-intensity ion implantation under conditions of a decrease or compensation of ion sputtering of the surface. An estimate of the effective diffusion coefficient from the Wagner relation for the layer growth rate $h = (2Dt)^{1/2}$ [29] gives a value for $h = 65\text{ }\mu\text{m}$ of about $5 \times 10^{-9}\text{ cm}^2/\text{s}$, which is much higher than the known literature data. So, for example,

in [26], when studying radiation-stimulated diffusion induced by a high current nitrogen ion beam with a density of 2 mA/cm^2 , even at a temperature of 500°C at an ion irradiation fluence of $3 \times 10^{19} \text{ ion/cm}^2$, the depth of nitrogen diffusion in AISI 420 steel was only $9\text{--}10 \text{ }\mu\text{m}$. This means that the diffusion coefficient of nitrogen in these experiments was many times lower. On the other hand, such depths of doping at lower current densities of nitrogen ions have not been achieved before. The authors of this article substantiated the possibility of a new mechanism of diffusion of dopants by numerical simulation and comparison with experiment. The mechanism is based on the fact that ion beams of low energy but high current density when interacting with metals, do not produce displacements of atoms, but cause the distribution of atom oscillation energies to deviate from thermodynamic equilibrium and also lead to the development of radiation-stimulated diffusion. The effect of deviation from thermodynamic equilibrium is determined by the intensity of the ion beam and the thermalization time of crystal lattice vibrations. It can be assumed that in our case, with a significant increase in the ion current density, a similar mechanism leads to a significant increase in the diffusion coefficient of implanted nitrogen.

An alternative version of high-intensity implantation with suppression of ion sputtering was studied in [30] using a hexagonal closed system simulating a hollow system for processing the inner surface. Ballistic focusing of the ion beam provided a divergent ion beam outside of its crossover.

The axially symmetric system significantly reduced the ion sputtering of the irradiated inner surface due to the deposition of sputter products from other parts of the cylinder. As a result, the conditions for diffusion saturation of the implanted inner surface of the hollow hexagon have been improved. The obtained results allowed us to conclude that this approach is promising for deep ion doping of the inner surfaces of holes and tubes with a length of several centimeters.

In general, the performed studies allow us to make several conclusions. First, repetitively-pulsed high-intensity nitrogen ion implantation under conditions of a decrease in surface ion sputtering or its compensation provides a significant increase in the efficient diffusion coefficient, which makes it possible to obtain deep ion-doped layers for shorter irradiation times. The depths of ion doping of steel with nitrogen, achieved in this work, are many times higher than the depths obtained during conventional nitriding or under conditions of high-current density ion implantation. Second, the reduction in surface ion sputtering makes it possible to increase the efficiency of implanted dopant accumulation and to reduce its influence on surface morphology. Data on measuring microhardness and wear resistance indicate the prospects for the use of high-intensity nitrogen ion implantation to improve the macroscopic properties of various metals and alloys.

4. Conclusions

Taking nitrogen implantation in AISI 420 steel as an example, the effect of ultrahigh-dose, high-intensity ion implantation at current densities up to 250 mA/cm^2 and ion irradiation fluences from 3.6×10^{20} to $4.5 \times 10^{21} \text{ ion/cm}^2$ at an ion energy of 1.6 keV was studied. It has been established that the depth of the ion-doped layer is determined by the competition between radiation-enhanced diffusion and ion sputtering of the surface. With an ion irradiation fluence of $4.5 \times 10^{21} \text{ ion/cm}^2$, the surface sputtering rate reached $83 \text{ }\mu\text{m/h}$, and the ion doping depth was about $50 \text{ }\mu\text{m}$. In the studied area, the coefficient of ion sputtering of steel by nitrogen ions changes in proportion to the ion current density and ion irradiation fluence. It has been experimentally established that a decrease in the ion sputtering coefficient of the surface due to a decrease in the energy of nitrogen ions from 1600 to 350 eV , while maintaining the ion current density, ion irradiation fluence and temperature mode of target irradiation, increases the ion-doped layer depth by more than three times from $25 \text{ }\mu\text{m}$ to $65 \text{ }\mu\text{m}$. The efficient diffusion coefficient at an ion doping depth of $65 \text{ }\mu\text{m}$, determined from the Wagner ratio, is more than two orders of magnitude higher than the data obtained when stainless steel is nitrided with an ion flux with a current density of about 1 mA/cm^2 .

Author Contributions: A.R.; scientific guidance and article writing, S.D., D.V. and A.G.; experimental investigation, O.K. and A.I.; processing of experimental results. All authors have read and agreed to the published version of the manuscript.

Funding: This research was funded by Ministry of Education and Science of the Russian Federation grant number FSWW-2023-0011.

Data Availability Statement: Not applicable.

Conflicts of Interest: The authors declare no conflict of interest.

References

- Deng, Y.; Chen, W.; Li, B.; Wang, C.; Kuang, T.; Li, Y. Physical vapor deposition technology for coated cutting tools: A review. *Ceram. Int.* **2020**, *46*, 18373–18390. [\[CrossRef\]](#)
- Libório, M.; Praxedes, G.; Lima, L.; Nascimento, I.; Sousa, R.; Naeem, M.; Costa, T.; Alves, S.; Iqbal, J. Surface modification of M2 steel by combination of cathodic cage plasma deposition and magnetron sputtered MoS₂-TiN multilayer coatings. *Surf. Coatings Technol.* **2020**, *384*, 125327. [\[CrossRef\]](#)
- Nascimento, I.O.; Naeem, M.; Freitas, R.S.; Nascimento, R.M.; Viana, B.C.; Sousa, R.R.M.; Feitor, M.C.; Iqbal, J.; Costa, T.H.C. Comparative study of structural and stoichiometric properties of titanium nitride films deposited by cathodic cage plasma deposition and magnetron sputtering. *Eur. Phys. J. Plus* **2022**, *137*, 319. [\[CrossRef\]](#)
- Gudmundsson, J.T.; Lundin, D. Introduction to magnetron sputtering. In *High Power Impulse Magnetron Sputtering*; Elsevier: Amsterdam, The Netherlands, 2020; pp. 1–48. [\[CrossRef\]](#)
- Khelifi, K.; Ben Cheikh Larbi, A.B.C. Investigation of adhesion of PVD coatings using various approaches. *Surf. Eng.* **2013**, *29*, 555–560. [\[CrossRef\]](#)
- Samanta, A.; Wang, Q.; Shaw, S.K.; Ding, H. Roles of chemistry modification for laser textured metal alloys to achieve extreme surface wetting behaviors. *Mater. Des.* **2020**, *192*, 108744. [\[CrossRef\]](#)
- Vorobyov, M.; Koval, T.; Shin, V.; Moskvina, P.; Tran, M.K.A.; Koval, N.; Ashurova, K.; Doroshkevich, S.; Torba, M. Controlling the Specimen Surface Temperature During Irradiation with a Submillisecond Electron Beam Produced by a Plasma-Cathode Electron Source. *IEEE Trans. Plasma Sci.* **2021**, *49*, 2550–2553. [\[CrossRef\]](#)
- Pimenov, V.N.; Borovitskaya, I.V.; Gribkov, V.A.; Demin, A.S.; Epifanov, N.A.; Maslyaev, S.A.; Morozov, E.V.; Sasinovskaya, I.P.; Bondarenko, G.G.; Gaydar, A.I.; et al. Influence of Pulsed Flows of Deuterium Ions and Deuterium Plasma on Cu–Ni and Cu–Ni–Ga Alloys. *J. Surf. Investig. X-ray Synchrotron Neutron Tech.* **2022**, *16*, 33–41. [\[CrossRef\]](#)
- Remnev, G.E.; Tarbokov, V.A.; Pavlov, S.K. Material Modification by Powerful Pulsed Ion Beams. *Inorg. Mater. Appl. Res.* **2022**, *13*, 626–640. [\[CrossRef\]](#)
- Pushilina, N.; Stepanova, E.; Syrtanov, M. Surface Modification of the EBM Ti-6Al-4V Alloy by Pulsed Ion Beam. *Metals* **2021**, *11*, 512. [\[CrossRef\]](#)
- Williams, J.; Poate, J. *Ion Implantation and Beam Processing*; Academic Press: Orlando, FL, USA, 1984. [\[CrossRef\]](#)
- Möller, W.; Parascandola, S.; Telbizova, T.; Günzel, R.; Richter, E. Surface processes and diffusion mechanisms of ion nitriding of stainless steel and aluminium. *Surf. Coatings Technol.* **2001**, *136*, 73–79. [\[CrossRef\]](#)
- Bandura, A.N.; Byrka, O.V.; Chebotarev, V.V.; Garkusha, I.E.; Makhaj, V.A.; Medvedev, V.; Taran, V.S.; Tereshin, V.I.; Skoblo, T.S.; Pugach, S.G. Alloying and modification of structural materials under pulsed plasma treatment. *Int. J. Plasma Environ. Sci. Technol.* **2011**, *5*, 2–6. [\[CrossRef\]](#)
- Huang, H.-H.; Liu, C.-F.; Wang, S.; Chen, C.-S.; Chang, J.-H. Nitrogen plasma immersion ion implantation treatment of Ti6Al7Nb alloy for bone-implant applications: Enhanced in vitro biological responses and in vivo initial bone-implant contact. *Surf. Coatings Technol.* **2021**, *405*, 126551. [\[CrossRef\]](#)
- Yushkov, G.Y.; Nikolaev, A.G.; Frolova, V.P.; Oks, E.M.; Roussikh, A.G.; Zhigalin, A.S. Multiply charged metal ions in high current pulsed vacuum arcs. *Phys. Plasmas* **2017**, *24*, 123501. [\[CrossRef\]](#)
- Torrisi, L.; Cutroneo, M.; Mackova, A.; Lavrentiev, V.; Pfeifer, M.; Krousky, E. An unconventional ion implantation method for producing Au and Si nanostructures using intense laser-generated plasmas. *Plasma Phys. Control. Fusion* **2016**, *58*, 025011. [\[CrossRef\]](#)
- Ryabchikov, A.I. High-Intensity Implantation with an Ion Beam's Energy Impact on Materials. *IEEE Trans. Plasma Sci.* **2021**, *49*, 2529–2534. [\[CrossRef\]](#)
- Anishchik, V.M.; Uglov, V.V. *Modifikatsiya Instrumental'nykh Materialov Ionnyimi I Plazmennymi Puchkami*; Belarusian State University: Minsk, Belarus, 2003; ISBN 985-445-906-3. (In Russian)
- Wei, R.; Wilbur, P.J.; Sampath, W.S.; Williamson, D.L.; Wang, L. Effects of Ion Implantation Conditions on the Tribology of Ferrous Surfaces. *J. Tribol.* **1991**, *113*, 166–173. [\[CrossRef\]](#)
- Wei, R.; Wilbur, P.; Ozturk, O.; Williamson, D. Tribological studies of ultrahigh dose nitrogen-implanted iron and stainless steel. *Nucl. Instruments Methods Phys. Res. Sect. B Beam Interactions Mater. Atoms* **1991**, *59–60*, 731–736. [\[CrossRef\]](#)
- Wei, R.; Wilbur, P.J.; Sampath, W.S.; Williamson, D.L.; Qu, Y.; Wang, L. Tribological Studies of Ion-Implanted Steel Constituents Using an Oscillating Pin-on-Disk Wear Tester. *J. Tribol.-Trans. ASME* **1990**, *112*, 27–34. [\[CrossRef\]](#)

22. Hutchings, R. A review of recent developments in ion implantation for metallurgical application. *Mater. Sci. Eng. A* **1994**, *184*, 87–96. [[CrossRef](#)]
23. Wei, R. Low energy, high current density ion implantation of materials at elevated temperatures for tribological applications. *Surf. Coatings Technol.* **1996**, *83*, 218–227. [[CrossRef](#)]
24. Ryabchikov, A.I.; Ananin, P.S.; Dektyarev, S.V.; Sivin, D.O.; Shevelev, A.E. High intensity metal ion beam generation. *Vacuum* **2017**, *143*, 447–453. [[CrossRef](#)]
25. Goncharenko, I.; Grigoriev, S.; Lopatin, I.; Koval, N.; Schanin, P.; Tukhfatullin, A.; Ivanov, Y.; Strumilova, N. Surface modification of steels by complex diffusion saturation in low pressure arc discharge. *Surf. Coatings Technol.* **2003**, *169–170*, 419–423. [[CrossRef](#)]
26. Byeli, A.V.; Vyblyi, Y.P.; Kukareko, V.A. Radiation-stimulated diffusion induced by high-current density nitrogen ion beam processing of steels. *Bull. Russ. Acad. Sci. Phys.* **2010**, *74*, 213–216. [[CrossRef](#)]
27. Behrish, R. *Sputtering by Particle Bombardment I*; Springer: Berlin/Heidelberg, Germany, 1983; p. 336.
28. Sigmund, P. Theory of Sputtering. I. Sputtering Yield of Amorphous and Polycrystalline Targets. *Phys. Rev.* **1969**, *184*, 383–416. [[CrossRef](#)]
29. Kofstad, P. *High-Temperature Oxidation of Metals*; Wiley: New York, NY, USA, 1996; p. 392.
30. Sivin, D.O.; Korneva, O.S.; Ivanova, A.I.; Vakhrushev, D.O. Gas-discharge plasma application for ion-beam treatment of the holes' inner surfaces. *J. Phys. Conf. Ser.* **2021**, *2064*, 012079. [[CrossRef](#)]

Disclaimer/Publisher's Note: The statements, opinions and data contained in all publications are solely those of the individual author(s) and contributor(s) and not of MDPI and/or the editor(s). MDPI and/or the editor(s) disclaim responsibility for any injury to people or property resulting from any ideas, methods, instructions or products referred to in the content.